

# Acoustic Anomaly Detection for Machine Sounds based on Image Transfer Learning

Robert Müller, Fabian Ritz, Steffen Illium and Claudia Linnhoff-Popien

Mobile and Distributed Systems Group, LMU Munich

{robert.mueller, fabian.ritz, steffen.illium, linnhoff}@ifi.lmu.de

## Abstract

In industrial applications, the early detection of malfunctioning factory machinery is crucial. In this paper, we consider acoustic malfunction detection via transfer learning. Contrary to the majority of current approaches which are based on deep autoencoders, we propose to extract features using neural networks that were pretrained on the task of image classification. We then use these features to train a variety of anomaly detection models and show that this improves results compared to convolutional autoencoders in recordings of four different factory machines in noisy environments. Moreover, we find that features extracted from ResNet based networks yield better results than those from AlexNet and SqueezeNet. In our setting, Gaussian Mixture Models and One-Class Support Vector Machines achieve the best anomaly detection performance.

**Index Terms:** Acoustic Anomaly Detection, Transfer Learning

## 1. Introduction

Anomaly detection is one of the most prominent industrial applications of machine learning. It is used for video surveillance, monitoring of critical infrastructure or the detection of fraudulent behavior. However, most of the current approaches are based on detecting anomalies in the visual domain. Issues arise when the scenery cannot be covered by cameras completely, leading to blind-spots in which no prediction can be made. Naturally, this applies to many internals of industrial production facilities and machines. In many cases a visual inspection can not capture the true condition of the surveilled entity. A pump suffering from a small leakage, a slide rail that has no grease or a fan undergoing voltage changes might appear intact when inspected visually but when monitored acoustically, reveal its actual condition through distinct sound patterns. Further, acoustic monitoring has the advantage of comparably cheap and easily deployable hardware. The early detection of malfunctioning machinery with a reliable acoustic anomaly detection system can prevent greater damages and reduce repair expenses.

In this work, we focus on the detection of anomalous sounds emitted from factory machinery such as fans, pumps, valves and slide rails. Obtaining an exhaustive number of recordings from anomalous operation is not appropriate as it would require either deliberately damaging machines or waiting a potentially long time until enough machines suffered from damages. Consequently, we assume there is no access to anomalous recordings during the training of the anomaly detection systems. Hence, training the system proceeds in a fully unsupervised manner. Moreover, we assume normal operation recordings to be contaminated with background noises from real world factory environments.

By observing that patterns of anomalous operation can often be spotted visually in the time-frequency representation of a recording, we conclude that pretrained image classification

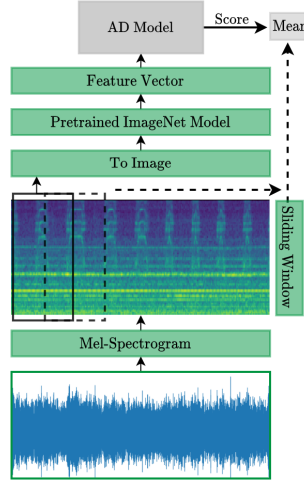


Figure 1: *Overview of the proposed workflow. First, the raw waveform is transformed into a Mel-spectrogram. Small segments of  $\approx 1s$  are then extracted in sliding window fashion. Subsequently, a pretrained image classification neural network is used to extract feature vectors. These feature vectors are then used to train an anomaly detection model. A prediction over the whole recording is made by averaging the scores of the analyzed segments.*

model can extract meaningful features. Although not trained on Mel-spectrogram images, these networks were shown to learn generic filters such as edge and object detectors. Moreover, this alleviates the burden of finding a suitable neural network architecture.

We propose to use features from images of segments gathered from Mel-spectrograms of normal operation data. We then standardize the obtained features and use them to train various anomaly detection models. A sliding window in combination with mean pooling is used to make a decision over a longer time horizon during inference (see Figure 1).

The remaining paper is structured as follows: In Section 2, we survey related approaches to acoustic anomaly detection in an unsupervised learning setting. Section 3 introduces the proposed approach with more mathematical rigor. Then we briefly introduce the dataset we used to evaluate our method in Section 4, followed by a description of the experimental setup in Section 5. Results are discussed in Section 6. We close by summarizing our findings and outlining future work in Section 7.

## 2. Related Work

While various approaches on classification [1, 2] and tagging [3] of acoustic scenes have been proposed in the last years,

acoustic anomaly detection is still underrepresented. Due to the release of publicly available datasets [4, 5, 6, 7], the situation is gradually improving.

The majority of current approaches relies on deep autoencoders (AE). An AE is a neural network (NN) that first compresses its input into a low dimensional representation and subsequently reconstructs the input. The reconstruction error is taken as the anomaly score since it is assumed that input differing from the training data cannot be reconstructed precisely.

Marchi et al. [8] use a bidirectional recurrent denoising AE to reconstruct auditory spectral features to detect novel events. Duman et al. propose to use a convolutional AE on Mel-spectrograms to detect anomalies in the context of industrial plants and processes. In [9], the authors compare various AE architectures with special focus on the applicability of these methods on the edge. They conclude that a convolutional architecture operating on the Mel-Frequency Cepstral coefficients is well suited for the task while a One-Class Support Vector Machine represents a strong and more parameter efficient baseline. Kawaguchi et al. [10] explicitly address the issue of background noise. An ensemble method of front-end modules and back-end modules followed by an ensemble-based detector combines the strengths of various algorithms. Front-ends consist of blind-dereverberation and anomalous-sound-extraction algorithms, back-ends are AEs. The final anomaly score is computed by score-averaging. Finally, in [11] anomalous sound detection is interpreted as statistical hypothesis testing where they propose a loss function based on the Neyman-Pearson lemma. However this approach relies on the simulation of anomalous sounds using expensive rejection sampling.

In contrast to these architecture-driven approaches, Koizumi et al. [12] introduced Batch-Uniformization, a modification to the AE’s training-procedure where the reciprocal of the probabilistic density of each sample is used to up-weigh rare sounds.

Another line of work investigates upon methods that operate directly on the raw waveform [13, 14]. These methods use generative, WaveNet-like [15] architectures to predict the next sample and take the prediction error as a measure of abnormality. Their results indicate a slight advantage over AE based approaches at the cost of higher computational demands.

In this work, we propose a different approach to acoustic anomaly detection. We use features extracted from NNs pre-trained with image classification to train anomaly detection models, which is inspired by the success of these features in other areas, such as snore sound classification [16], emotion recognition in speech [17], music information retrieval [18] and medical applications [19].

### 3. Proposed Approach

Let  $X \in \mathbb{R}^{F \times T}$  be the time-frequency representation of some acoustic recording where  $T$  is the time dimension and  $F$  the number of frequency bins. In the context of acoustic anomaly detection, we want to find a function  $\mathcal{F} : X \rightarrow \mathbb{R}$  such that  $\mathcal{F}(X)$  is higher for anomalous recordings than for recordings from normal operation without having access to anomalous recordings during training. To reduce computational demands and to increase the number of datapoints, it is common to extract smaller patches  $x_1, \dots, x_i, \dots, x_n$  of the underlying spectrogram  $X$  across the time dimension in a sliding window fashion where  $x_i \in \mathbb{R}^{t \times F}$ ,  $t < T$ . Here we propose to extract a  $d$ -dimensional feature vector using a feature extractor  $f : \mathbb{R}^{t \times F} \rightarrow \mathbb{R}^d$  for each  $x_i$ . Then we can set  $\mathcal{F}$  to be some anomaly detection algorithm and train  $\mathcal{F}$  on all features of

extracted patches in the dataset  $\mathcal{D} = \{X_j \in \mathbb{R}^{F \times T}\}_{j=1}^N$ . The anomaly score for the entire spectrogram  $X$  can be computed by averaging (mean-pooling) the predictions from the smaller patches:

$$\mathcal{F}(X) = \frac{1}{n} \sum_{i=1}^n \mathcal{F} \circ f(x_i)$$

Since we observed that acoustic anomalies of factory machinery can often be spotted visually (see Figure 2), we claim that a NN pretrained on the task of image recognition can extract meaningful features that help to distinguish between normal and anomalous operation. The filters of these networks were shown [20, 21] to having learned to recognize colors, contrast, shapes (e.g. lines, edges), objects and textures. Leveraging pre-trained NNs is commonly referred to as transfer learning.

## 4. Dataset

In our experiments, we use the recently introduced *MIMII* dataset [5]. It consists of recordings from four industrial machine types (fans, pumps, slide rails and valves) under normal and anomalous operation. For each machine type, four datasets exist, each representing a different product model. Note that anomalous recordings exhibit various scenarios such as leakage, clogging, voltage change, a loose belt or no grease. In addition, background noise recorded in real-world factories was added to each recording according to a certain Signal-to-Noise-Ratio (SNR). In our analysis, we use sounds with a SNR of  $-6\text{dB}$ . We argue that this is very close to the practical use as it is unpreventable that microphones monitoring machines will also capture background noises in a factory environment. Each single-channel recording is 10 seconds long and has a sampling rate of 16kHz. Figure 2 depicts Mel-spectrograms of normal and anomalous sounds for all machine types.

## 5. Experiments

To study the efficacy of image transfer learning for acoustic anomaly detection, we first compute the Mel-Spectrograms for all recordings in the dataset using 64 Mel-bands, a hanning window of 1024 and a hop length of 256. Afterwards, we extract  $64 \times 64$  Mel-spectrogram patches ( $\approx 1\text{s}$ ) in a sliding window fashion with an offset of 32 across the time axis and convert them to RGB-images utilizing the *viridis* color-map. Subsequently, images are up-scaled and normalized to match the domain of the feature extractor  $f$ . Note that due to our choice of the size of Mel-spectrogram patches, the original aspect-ratio remains unaltered, countering potential information loss. Then, we extract a feature vector for each patch by using various NNs that were pretrained on ImageNet and apply standardization. Finally, we train multiple anomaly detection models on these features. During training, we randomly exclude 150 samples, each with a length of 10s, from the normal data for testing. The same amount of anomalous operation data is randomly added to the test set. A decision for each sample is made using mean pooling, as discussed in Section 3. The whole process is repeated 5 times with 5 different seeds and the average *Area Under the Receiver Operating Characteristic Curve* (AUC) is used to report performance.

### 5.1. Pretrained Feature Extractors

Convolutional Neural Networks (CNNs) are known to perform well on two dimensional data input with spatial relations.

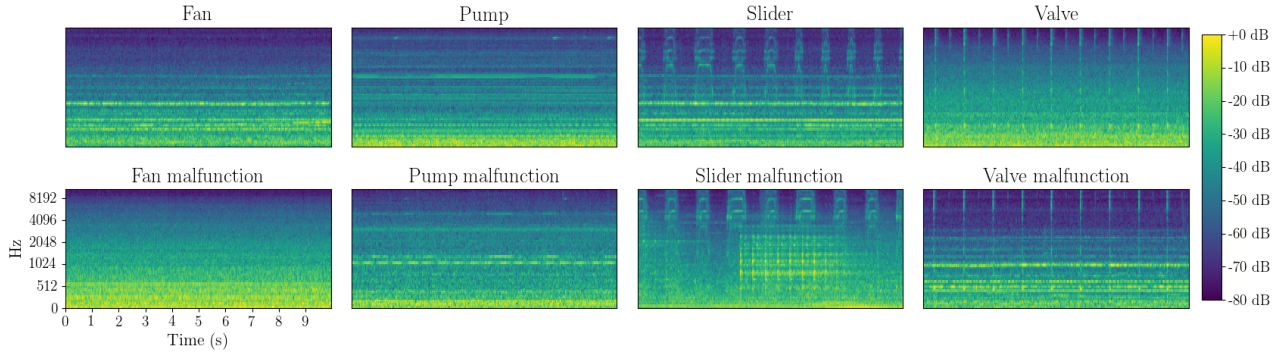


Figure 2: Mel-spectrograms of recordings from normal (top row) and anomalous operation (bottom row) across all machine types in the MIMII dataset. Since anomalies can often be spotted visually in this representation, using image classification models is reasonable.

Hence, we repurpose the following classifiers, pretrained on ImageNet [22] for feature extraction:

*Alexnetv3* [23] is a two stream network architecture involving convolutions (kernels:  $11 \times 11$ ,  $5 \times 5$  and  $3 \times 3$ ) and max pooling followed by two fully connected layers. We use the activations from the penultimate layer, resulting in a 4096 dimensional vector.

*ResNet18* [24] was designed to counter the problem of diminishing returns when network depth increases. The architecture consists of multiple residual blocks. 16 + 2 layers (initial convolution and max-pooling, followed by 8 convolutional residual blocks) with increasing convolutional filter sizes lead to a single average pooling operation. We use the 512 activations thereafter for training.

*ResNet34* [24] adheres to the same principles as *ResNet18* at an increased depth of  $32 + 2$  layers.

*SqueezeNet* [25] was designed to use as few parameters as possible (50 times fewer than AlexNet) while still providing comparable classification accuracy. *Fire* modules equipped with *squeeze* ( $1 \times 1$ ) and *expand* ( $3 \times 3$ ) layers. In addition, we apply  $2 \times 2$  average pooling to the final convolution to extract a 2048-dimensional feature vector.

## 5.2. Anomaly Detection Models

We compare six well established anomaly detection algorithms: The *Isolation Forest (IF)* [26] is based upon the assumption that anomalies are easier to isolate in feature space. Features are randomly partitioned and the average path length across multiple trees is used as the normality score. We set the number of trees in the forest to 128.

A *Gaussian Mixture Model (GMM)* fits a mixture of Gaussians on to the observed features. The log-probability of a feature vector under the trained GMM is used as the normality score. Parameters are estimated via expectation-maximization. We use 80 mixture components with diagonal covariance matrix initialized using k-means. The iteration limit is set to 150.

The *Bayesian Gaussian Mixture Model (B-GMM)* is additionally trained via variational inference and places prior distributions over the parameters. In many cases, it is less dependent on the specified number of mixtures. In our setting, this might be advantageous as this quantity is hard to determine due to the lack of anomalous data for validation. We use the same parameters as for the GMM.

A *One-Class Support Vector Machine (OC-SVM)* [27] aims to find the maximum margin hyperplane that best separates the

data from the center. As  $\nu$  (approximate ratio of outliers) must be  $> 0$ , we set  $\nu = 10^{-4}$  since the training data consists of normal data only.

*Kernel Density Estimation (KDE)* is a non-parametric density estimation algorithm that centers a predefined kernel with some bandwidth over each datapoint and increases the density around this point. Areas with many datapoints will therefore have a higher density than those with only a few. We use a gaussian kernel with a bandwidth of 0.1. The density at a datapoint is used as normality score.

A *Deep Convolutional Autoencoder (DCAE)* reconstructs its own input, in this case the Mel-spectrogram images. We use a LeNet style, three layer convolutional encoder architecture with 32, 64 and 128 output channels, a kernel size of 5, ELU [28] activation functions, batch normalization and a 128-dimensional bottleneck (LeNet-AE). Moreover, we also consider a simpler encoder architecture with 12, 24 and 48 output channels, ReLU [29] activation functions and a kernel size of 4 (Small-DCAE). The decoders mirror the encoders using de-convolutional layers. For optimization, we use Adam with learning rate =  $10^{-4}$ , batch size = 128 and train for 80 epochs. The mean squared error between the original image and the reconstruction is used as the loss function and anomaly score.

## 6. Results

In this section, we discuss the key findings of the results depicted in Table 1. These findings refer to the setting introduced in the prior chapters and we do not claim them to hold in arbitrary cases.

### 1) Image Transfer Learning is more effective for detecting anomalous machine sounds than autoencoders trained from scratch.

Autoencoders outperform the models based on image transfer learning only in a single setting (Small-DCAE on Pump-M6) and in the majority of the cases, LeNet-DCAE yields better results than Small-DCAE. Mostly, the DCAEs do not even come close to their competitors, which supports our hypothesis that the features extracted by learned filters from pretrained image classification models are better suited for detecting subtle anomalies. This might be explained by reconstruction based anomaly detection being based upon a proxy task rather than modeling the task explicitly.

### 2) ResNet architectures are superior feature extractors.

To compare the feature extractors, we count the scenarios

Table 1: *Anomaly detection results for all machine types and machine IDs. The best performing model (read vertically) is written in bold and colored in green, the second best is underlined and colored in yellow. Each entry is an average AUC across five seeds.*

		Fan				Pump				Slider				Valve			
		M0	M2	M4	M6												
AlexNet	GMM	57.7	61.7	53.9	<b>94.5</b>	84.1	<b>70.8</b>	81.6	66.0	98.3	80.9	61.4	57.5	60.2	69.2	59.9	53.5
	B-GMM	50.9	61.4	47.7	82.2	71.8	60.2	73.4	53.3	83.2	65.0	50.0	57.0	55.2	62.7	51.4	48.3
	IF	53.1	59.7	48.9	84.6	75.9	62.4	75.0	55.9	89.4	69.0	51.9	56.2	50.1	63.4	53.3	49.8
	KDE	55.7	59.1	50.5	90.3	76.4	65.9	74.8	61.0	97.8	79.3	59.7	55.0	54.6	64.4	57.1	51.4
	OC-SVM	51.0	<b>73.1</b>	<b>59.7</b>	93.2	77.5	56.4	81.1	60.1	96.2	81.4	53.6	56.5	61.6	73.6	48.3	48.9
ResNet18	GMM	<b>62.6</b>	64.1	59.3	<b>94.4</b>	<b>84.5</b>	<b>71.3</b>	84.0	<b>68.3</b>	99.1	<b>85.8</b>	68.8	65.6	58.3	73.3	60.2	56.9
	B-GMM	<b>59.2</b>	60.5	54.8	91.0	79.1	69.7	79.4	59.5	98.3	77.7	61.4	61.2	70.1	71.7	56.1	50.3
	IF	58.0	60.5	55.3	86.5	70.8	59.0	77.3	54.6	97.7	72.7	60.6	61.2	56.5	69.8	58.2	47.5
	KDE	57.9	59.1	55.6	85.9	76.6	56.5	76.7	62.2	98.1	77.0	61.2	60.9	57.6	62.9	56.8	49.7
	OC-SVM	55.0	<b>68.8</b>	57.4	87.7	71.6	55.2	78.6	60.6	96.7	79.6	69.3	66.2	61.1	76.1	56.8	43.1
ResNet34	GMM	58.7	65.6	57.0	90.9	78.4	66.8	<b>87.9</b>	63.2	<b>99.6</b>	<b>90.4</b>	<b>82.5</b>	69.1	<b>73.0</b>	<b>79.1</b>	60.1	<b>61.9</b>
	B-GMM	55.7	61.8	52.3	85.8	71.5	61.1	84.5	55.2	<b>99.2</b>	85.4	<b>72.3</b>	63.6	70.8	76.2	59.3	57.9
	IF	53.9	62.0	49.9	82.2	52.3	48.3	79.3	49.4	98.6	83.1	69.5	60.2	65.9	71.2	<b>60.3</b>	54.0
	KDE	55.0	62.6	52.3	83.1	62.0	51.8	82.8	58.3	99.0	84.0	68.2	62.2	67.5	71.9	53.9	58.2
	OC-SVM	50.1	67.4	57.5	83.0	64.9	51.5	81.2	60.2	96.8	85.0	71.4	64.3	<b>75.6</b>	<b>77.8</b>	<b>64.3</b>	53.1
SqueezeNet	GMM	56.1	60.4	49.4	83.4	72.1	46.4	87.6	60.8	96.7	76.8	52.1	62.9	62.8	75.3	53.3	57.3
	B-GMM	54.4	59.8	47.0	84.5	72.3	48.2	86.2	69.0	95.0	78.8	55.8	65.0	63.8	74.0	52.4	56.8
	IF	53.2	64.0	44.8	84.6	76.1	45.5	85.3	60.2	98.9	78.2	53.1	<b>70.6</b>	56.6	68.7	51.5	56.6
	KDE	54.4	60.5	47.0	84.3	74.5	45.2	86.5	61.4	98.7	80.8	56.4	69.2	65.0	74.5	52.8	57.7
	OC-SVM	55.6	64.8	46.2	86.7	78.8	49.4	<b>88.4</b>	62.3	99.2	81.5	59.4	<b>71.6</b>	69.0	71.3	53.1	<b>58.2</b>
LeNet-DCAE	-	49.1	57.0	53.2	66.9	65.3	54.4	76.0	66.6	95.9	70.4	56.2	50.6	42.3	55.6	51.2	45.5
Small-DCAE	-	48.3	54.1	49.3	63.7	69.9	52.9	73.1	<b>69.2</b>	95.3	68.4	55.7	53.3	36.6	57.2	51.2	45.4

in that a specific feature extractor combined with different anomaly detection models yields the highest or the second highest score and create tuples of the form (1<sup>st</sup>, 2<sup>nd</sup>). As depicted in Table 1, there are 16 distinct evaluation settings in which either the highest or the second highest score can be achieved. Ranked from best to worst, we get the following results: ResNet34 (6, 6), ResNet18 (3, 5), AlexNet (3, 2), SqueezeNet (2, 2) and Autoencoders (1, 0). A clear superiority of ResNet based feature extractors can be observed. Interestingly, these are also the models with a lower classification error on ImageNet compared to SqueezeNet and AlexNet. These results are consistent with a recent finding that there is strong correlation between ImageNet top-1 accuracy and transfer accuracy [30]. Another important observation is that ResNet34’s good performance almost exclusively stems from top performance on sliders and valves. The Mel-spectrogram images from these machines have more fine granular variations than those from fans and pumps which show a more stationary allocation of frequency bands. We assume that ResNet34 extracts features on a more detailed level which can explain inferior performance on fan and pump data. Generally, we have found SqueezeNet to be the least reliable feature extractor. Note that these findings also hold when all feature vectors are adjusted to the same dimensionality using PCA.

### 3) GMM and OC-SVM yield the best performance.

To compare the anomaly detection models, we count the scenarios in that a specific anomaly detection model combined with different feature extractors achieves the best or second best result. Employing the same ranking strategy as above, the results are as follows: GMM (9, 8), OC-SVM (6, 2), Autoencoders (1, 0), B-GMM (0, 3), IF (0, 2), KDE (0, 0). Clearly, GMM and OC-SVM outperform all other models by a large margin. Together, they account for 15/16 of the best performing models and 10/16 of second best performing

models. Although GMM and B-GMM are both based on the same theoretical assumptions, B-GMM produces inferior results. We suspect the weight priors to potentially be too restrictive.

### 4) Results are highly dependent on the machine type and the machine model.

The model performing best on valves has an average AUC of 79.1. This is low compared to the other machine types as these always have at least one scenario with an average AUC > 80. Moreover, the highest achieved score varies considerably across all machine types. This indicates that some machine types are more suited for our approach (pumps, sliders) than others (fans, valves). More importantly, a significant variance between different machine IDs (M1 - M6) can be observed. Results on fans make this problem most evident. While M1, M2 and M4 have average scores of 62, 6, 73.1 and 59.7, M6 achieves an average of 94.5. M6 improves upon M4 at ≈ 30%. This suggests that anomalous sound patterns are vastly different (more or less subtle) even for different models of the same machine type. Future approaches should take this into account.

## 7. Conclusion

In this work, we thoroughly studied acoustic anomaly detection for machine sounds. For feature extraction, we used readily available neural networks that were pretrained on ImageNet. We then used these features to train five different anomaly detection models. Results indicate that features extracted with ResNet based architectures yield the best average AUC in combination with a GMM or OC-SVM. Future work could investigate upon further ensemble approaches and other feature extraction architectures [10, 31, 32, 33]. In addition, our approach might benefit from techniques to reduce background noise [34] or to enable decisions over a longer time-horizon [35].

## 8. References

[1] A. Mesaros, T. Heittola, and T. Virtanen, “A multi-device dataset for urban acoustic scene classification,” in *Proceedings of the Detection and Classification of Acoustic Scenes and Events 2018 Workshop (DCASE2018)*, November 2018, pp. 9–13. [Online]. Available: <https://arxiv.org/abs/1807.09840>

[2] J. Abeßer, “A review of deep learning based methods for acoustic scene classification,” *Applied Sciences*, vol. 10, no. 6, 2020.

[3] E. Fonseca, M. Plakal, F. Font, D. P. W. Ellis, and X. Serra, “Audio tagging with noisy labels and minimal supervision,” in *Submitted to DCASE2019 Workshop*, NY, USA, 2019.

[4] Y. Jiang, C. Li, N. Li, T. Feng, and M. Liu, “Haasd: A dataset of household appliances abnormal sound detection,” in *Proceedings of the 2018 2nd International Conference on Computer Science and Artificial Intelligence*, ser. CSAI 18. New York, NY, USA: Association for Computing Machinery, 2018, p. 610.

[5] H. Purohit, R. Tanabe, K. Ichige, T. Endo, Y. Nikaido, K. Suefusa, and Y. Kawaguchi, “Mimi dataset: Sound dataset for malfunctioning industrial machine investigation and inspection,” *arXiv preprint arXiv:1909.09347*, 2019.

[6] Y. Koizumi, S. Saito, H. Uematsu, N. Harada, and K. Imoto, “Toyadmos: A dataset of miniature-machine operating sounds for anomalous sound detection,” in *2019 IEEE Workshop on Applications of Signal Processing to Audio and Acoustics (WASPAA)*. IEEE, 2019, pp. 313–317.

[7] S. Grollmisch, J. Abeßer, J. Liebetrau, and H. Lukashevich, “Sounding industry: Challenges and datasets for industrial sound analysis,” in *2019 27th European Signal Processing Conference (EUSIPCO)*. IEEE, 2019, pp. 1–5.

[8] E. Marchi, F. Vesperini, F. Ebyen, S. Squartini, and B. Schuller, “A novel approach for automatic acoustic novelty detection using a denoising autoencoder with bidirectional lstm neural networks,” in *2015 IEEE international conference on acoustics, speech and signal processing (ICASSP)*. IEEE, 2015, pp. 1996–2000.

[9] M. Meire and P. Karsmakers, “Comparison of deep autoencoder architectures for real-time acoustic based anomaly detection in assets,” in *2019 10th IEEE International Conference on Intelligent Data Acquisition and Advanced Computing Systems: Technology and Applications (IDAACS)*, vol. 2, 2019, pp. 786–790.

[10] Y. Kawaguchi, R. Tanabe, T. Endo, K. Ichige, and K. Hamada, “Anomaly detection based on an ensemble of dereverberation and anomalous sound extraction,” in *ICASSP 2019 - 2019 IEEE International Conference on Acoustics, Speech and Signal Processing (ICASSP)*, 2019, pp. 865–869.

[11] Y. Koizumi, S. Saito, H. Uematsu, and N. Harada, “Optimizing acoustic feature extractor for anomalous sound detection based on neyman-pearsor lemma,” in *2017 25th European Signal Processing Conference (EUSIPCO)*. IEEE, 2017, pp. 698–702.

[12] Y. Koizumi, S. Saito, M. Yamaguchi, S. Murata, and N. Harada, “Batch uniformization for minimizing maximum anomaly score of dnn-based anomaly detection in sounds,” in *2019 IEEE Workshop on Applications of Signal Processing to Audio and Acoustics (WASPAA)*, 2019, pp. 6–10.

[13] T. Hayashi, T. Komatsu, R. Kondo, T. Toda, and K. Takeda, “Anomalous sound event detection based on wavenet,” in *2018 26th European Signal Processing Conference (EUSIPCO)*. IEEE, 2018, pp. 2494–2498.

[14] E. Rushe and B. M. Namee, “Anomaly detection in raw audio using deep autoregressive networks,” in *ICASSP 2019 - 2019 IEEE International Conference on Acoustics, Speech and Signal Processing (ICASSP)*, 2019, pp. 3597–3601.

[15] A. v. d. Oord, S. Dieleman, H. Zen, K. Simonyan, O. Vinyals, A. Graves, N. Kalchbrenner, A. Senior, and K. Kavukcuoglu, “Wavenet: A generative model for raw audio,” *arXiv preprint arXiv:1609.03499*, 2016.

[16] S. Amiriparian, M. Gerczuk, S. Ottl, N. Cummins, M. Freitag, S. Pugachevskiy, A. Baird, and B. W. Schuller, “Snore sound classification using image-based deep spectrum features.” in *INTERSPEECH*, vol. 434, 2017, pp. 3512–3516.

[17] N. Cummins, S. Amiriparian, G. Hagerer, A. Batliner, S. Steidl, and B. W. Schuller, “An image-based deep spectrum feature representation for the recognition of emotional speech,” in *Proceedings of the 25th ACM international conference on Multimedia*, 2017, pp. 478–484.

[18] G. Gwardys and D. Grzywczak, “Deep image features in music information retrieval,” *International Journal of Electronics and Telecommunications*, vol. 60, no. 4, pp. 321–326, 2014.

[19] S. Amiriparian, M. Schmitt, S. Ottl, M. Gerczuk, and B. Schuller, “Deep unsupervised representation learning for audio-based medical applications,” in *Deep Learners and Deep Learner Descriptors for Medical Applications*, L. Nanni, S. Brahnam, S. Ghidoni, R. Brattin, and L. Jain, Eds., im Druck / in print.

[20] C. Olah, A. Mordvintsev, and L. Schubert, “Feature visualization,” *Distill*, vol. 2, no. 11, p. e7, 2017.

[21] C. Olah, N. Cammarata, L. Schubert, G. Goh, M. Petrov, and S. Carter, “An overview of early vision in inceptionv1,” *Distill*, vol. 5, no. 4, pp. e00024–002, 2020.

[22] J. Deng, W. Dong, R. Socher, L.-J. Li, K. Li, and L. Fei-Fei, “ImageNet: A Large-Scale Hierarchical Image Database,” in *CVPR09*, 2009.

[23] A. Krizhevsky, I. Sutskever, and G. E. Hinton, “Imagenet classification with deep convolutional neural networks,” in *Advances in neural information processing systems*, 2012, pp. 1097–1105.

[24] K. He, X. Zhang, S. Ren, and J. Sun, “Deep residual learning for image recognition,” in *Proceedings of the IEEE conference on computer vision and pattern recognition*, 2016, pp. 770–778.

[25] F. N. Iandola, S. Han, M. W. Moskewicz, K. Ashraf, W. J. Dally, and K. Keutzer, “SqueezeNet: Alexnet-level accuracy with 50x fewer parameters and < 0.5 mb model size,” *arXiv preprint arXiv:1602.07360*, vol. 1, no. 10, 2016.

[26] F. T. Liu, K. M. Ting, and Z. Zhou, “Isolation forest,” in *2008 Eighth IEEE International Conference on Data Mining*, 2008, pp. 413–422.

[27] B. Schölkopf, R. C. Williamson, A. J. Smola, J. Shawe-Taylor, and J. C. Platt, “Support vector method for novelty detection,” in *Advances in neural information processing systems*, 2000, pp. 582–588.

[28] D.-A. Clevert, T. Unterthiner, and S. Hochreiter, “Fast and accurate deep network learning by exponential linear units (elus). arxiv 2015,” *arXiv preprint arXiv:1511.07289*, 2 2016.

[29] V. Nair and G. E. Hinton, “Rectified linear units improve restricted boltzmann machines,” in *Proceedings of the 27th international conference on machine learning (ICML-10)*, 2010, pp. 807–814.

[30] S. Kornblith, J. Shlens, and Q. V. Le, “Do better imagenet models transfer better?” in *Proceedings of the IEEE conference on computer vision and pattern recognition*, 2019, pp. 2661–2671.

[31] J. Pons and X. Serra, “musicnn: Pre-trained convolutional neural networks for music audio tagging,” *arXiv preprint arXiv:1909.06654*, 2019.

[32] A. G. Howard, M. Zhu, B. Chen, D. Kalenichenko, W. Wang, T. Weyand, M. Andreetto, and H. Adam, “Mobilenets: Efficient convolutional neural networks for mobile vision applications,” *arXiv preprint arXiv:1704.04861*, 2017.

[33] G. Huang, Z. Liu, K. Weinberger, and L. van der Maaten, “Densely connected convolutional networks. arxiv 2017,” *arXiv preprint arXiv:1608.06993*, 2016.

[34] X. Zhang, X. Zhou, M. Lin, and J. Sun, “Shufflenet: An extremely efficient convolutional neural network for mobile devices,” in *Proceedings of the IEEE conference on computer vision and pattern recognition*, 2018, pp. 6848–6856.

[35] W. Xie, A. Nagrani, J. S. Chung, and A. Zisserman, “Uttterance-level aggregation for speaker recognition in the wild,” in *ICASSP 2019-2019 IEEE International Conference on Acoustics, Speech and Signal Processing (ICASSP)*. IEEE, 2019, pp. 5791–5795.